Available online at www.sciencedirect.com
SCIENCE DIRECT®
PERGAMON
Polyhedron 22 (2003) 1271–1279
POLYHEDRON
www.elsevier.com/locate/poly

Trinuclear complexes of a series of 'tritopic' hydrazide ligands—structural and magnetic properties

Victoria A. Milway, Liang Zhao, Tareque S.M. Abedin, Laurence K. Thompson *, Zhiqiang Xu

Department of Chemistry, Memorial University of Newfoundland, St. John's, Nfld, Canada A1B 3X7

Received 5 November 2002; accepted 31 January 2003

Abstract

Copper(II) and manganese(II) complexes of some new symmetric and asymmetric tritopic hydrazide ligands based on 2,6-pyridine-dihydrazide (L1, L2) and iminodiacetic acid dihydrazide (L3) have been studied. The linear trinuclear complexes $[Cu_3(L1\text{-}3H)(CH_3COO)_3(H_2O)_2]\cdot H_2O$ (**1**) and $[Cu_3(L2\text{-}4H)(H_2O)_3(CH_3OH)](NO_3)_2$ (**3**) have three copper(II) centers bridged by *trans*-N–N diazine linkages and exhibit moderate antiferromagnetic exchange. The complex $[Mn_3(L3)_2(CH_3CN)_2(H_2O)_2](ClO_4)_6\cdot 2H_2O$ (**5**) has an unusual trinuclear structure involving an alkoxy-bridged dinuclear center and an essentially isolated mononuclear Mn(II) center. The Mn(II) ions are antiferromagnetically coupled within the dinuclear subunit. Structural and magnetic data are discussed.

Keywords: Trinuclear complexes; Tritopic hydrazide ligands; Structural property; Magnetic property

1. Introduction

Symmetric 'tritopic' ligands, e.g. 2-poap (Scheme 1), based on a central pyridine-2,6-dicarboxylic acid hydrazide core, have been successfully used to create self-assembled $[3 \times 3]$ M_9 (M = Mn(II), Cu(II)) square grid structures, with novel structural and magnetic properties [1–5]. Such grids are formed generally with metal salts with weakly coordinating anions (e.g. NO_3^-, ClO_4^-, BF_4^-, etc.) and the metal centers occupy the ligand pockets in a linear, contiguous fashion with alkoxide bridges (Scheme 1). However, in the presence of more strongly coordinating anions, e.g. acetate, and strong donor solvent molecules, e.g. DMF, DMSO, grid formation is inhibited in the copper(II) case and linear trinuclear complexes are formed [6,7]. The three copper(II) ions in these compounds are coordinated in a different manner with the *trans*-N–N diazine ligand fragments bridging the metal centers (Scheme 1). Magnetic coupling occurs between the copper(II) centers via the N–N bridges with dominant antiferromagnetic exchange.

In the current report, a series of modified tritopic ligands (L1–L3) has been synthesized and their copper(II) and manganese(II) complexes studied. In each case, the ligands form trinuclear Cu(II) complexes, in which the ligand pockets adopt a *trans* conformation about the diazine N–N bonds, which bridge the three metal centers. Crystal structures have been carried out on $[Cu_3(L1\text{-}3H)(CH_3COO)_3(H_2O)_2]\cdot H_2O$ (**1**) and $[Cu_3(L2\text{-}4H)(H_2O)_3(CH_3OH)](NO_3)_2$ (**3**), which have trinuclear Cu_3 subunits with the *trans*-N–N bridged structure. Structural data on the complex $[Mn_3(L3)_2(CH_3CN)_2(H_2O)_2](ClO_4)_6\cdot 2H_2O$ (**5**) reveals a trinuclear structural arrangement, involving a dinuclear and an essentially isolated mononuclear Mn(II) center, while $[Mn(L1)(NO_3)_2(H_2O)_2]\cdot 2H_2O$ (**6**) is a mononuclear derivative. Variable-temperature magnetic studies have been carried out on these and other similar complexes, and are discussed in relation to the structures and the bridging groups present.

* Corresponding author. Tel.: +1-709-737-8750; fax: +1-709-737-3702.
E-mail address: lthomp@mun.ca (L.K. Thompson).

0277-5387/03/$ - see front matter
doi:10.1016/S0277-5387(03)00069-X

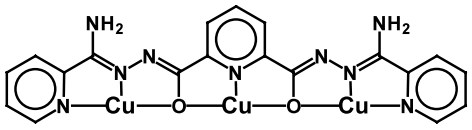

2poap

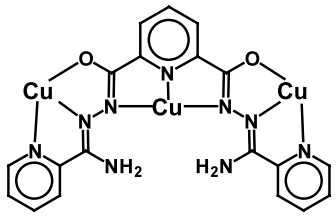

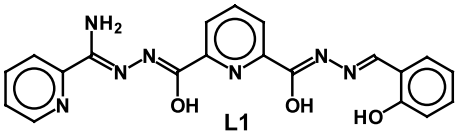

L1

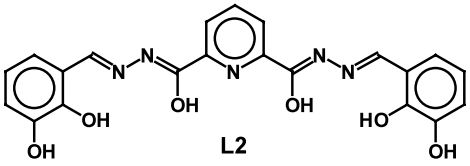

L2

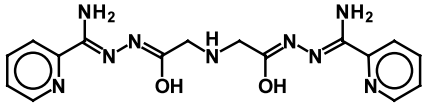

L3

Scheme 1.

2. Experimental

2.1. Physical measurements

Infrared spectra were recorded as Nujol mulls using a Mattson Polaris FTIR instrument. UV–Vis spectra were obtained as Nujol mulls with a Cary 5E spectrometer. Mass spectra were obtained using a VG micromass 7070HS spectrometer. C, H, N analyses on vacuum-dried samples were performed by the Canadian Microanalytical Service, Delta, BC, Canada. Variable-temperature magnetic data were obtained with a Quantum Design MPMS5S SQUID magnetometer operating at 0.1 T in DC mode. Calibrations were carried out using a palladium standard cylinder. Diamagnetic corrections for the sample holder and diamagnetic components of the complexes were applied.

2.2. Synthesis of the ligands

2.2.1. 2,6-Pyridine dicarboxylic acid hydrazide ligand L1

The 2,6-pyridine-bis-methylcarboxylate (Scheme 2, a) (19.8 g, 0.102 mol) was dissolved in warm methanol (500 ml) with stirring. Anhydrous hydrazine (3.20 g, 0.100 mol) was dissolved in methanol (100 ml) and added dropwise to the stirred diester solution over a period of 18 h. A white crystalline solid formed during the reaction, which was filtered off, washed with methanol and dried under vacuum. This product is a mixture according to mass spectral data, containing the desired mono-hydrazide (Scheme 2, b) and also the dihydrazide (Scheme 2, c). The crude product (b+c; 10.1 g) was added to a solution of pyridine-2-iminoacetate (12.5 g, 0.092 mol) in methanol (150 ml), obtained from the reaction of 2-cyanopyridine (9.6 g) with sodium methoxide and a few drops of glacial acetic acid, and the mixture refluxed for 2 h. Cooling to room temperature produced a white powder, identified as the di-substituted ligand 2-poap (Scheme 1), which was separated by filtration. The volume of the filtrate was reduced under vacuum and diethyl ether added producing a fine yellow powder (Scheme 2, d), which was filtered off (yield: 9.5 g). IR (cm^{-1}) 3407, 3332 (NH), 1719, 1690 (ester C=O), 997 (py). Mass spectrum (major mass peaks, *m*/*z*): 300 [M+H] 282, 223, 163, 107 and 79.

Hydrazine (1.84 g, 0.058 mol) was dissolved in methanol (150 ml), and the solution cooled in an ice bath. Intermediate d (7.65 g, 0.0256 mol) was added and the mixture stirred for 20 min. The ice bath was removed and the stirring continued overnight. The resulting white solid (Scheme 2, e) was collected by filtration and washed with methanol (yield: 68%). IR (cm^{-1}) 3422, 3275 (NH), 1650 (C=O), 999 (py). Mass spectrum (major mass peaks, *m*/*z*): 299 [M], 281, 195, 137, 107 and 78.

Salicylaldehyde (2.06 g, 0.017 mol) was added to a suspension of 2e (3.01 g, 0.010 mol) in methanol (100 ml) and the mixture refluxed overnight. A pale yellow powder (L1) formed, which was filtered off and washed with methanol (yield: 78%). m.p. 240–242 °C. Mass spectrum (major mass peaks): 403 [M], 385, 266, 223, 194 and 78. Elemental analysis: (L1) Anal. Found: C, 58.51; H, 3.64; N, 23.50. Calc. for $C_{20}H_{17}N_7O_3 \cdot 0.5H_2O$: C, 58.25; H, 4.40; N, 23.77%.

2.2.2. 2,6-Pyridine dicarboxylic acid hydrazide ligand L2

2,6-Pyridine dihydrazide (1.95 g, 0.010 mol) and 2,3-dihydroxybenzaldehyde (2.76 g, 0.020 mol) were reacted together in refluxing methanol (80 ml) for 8 h. A pale yellow solid formed on cooling (yield: 92%). m.p. (dec.) > 300 °C. Mass spectrum (major mass peaks, *m*/*z*): 195. No higher mass peaks were observed under any conditions. This peak corresponds to 2,6-pyridine dihydrazide, which appears to result from cleavage at the Schiff base C=N sites. IR (cm^{-1}) 3314 (m), 1684 (sh), 1667 (s), 1608 (w). Elemental analysis: (L2) Anal. Found: C, 54.75; H, 4.16; N, 15.13. Calc. for $C_{21}H_{15}N_5O_6 \cdot 1.5H_2O$: C, 54.55; H, 4.36; N, 15.14%.

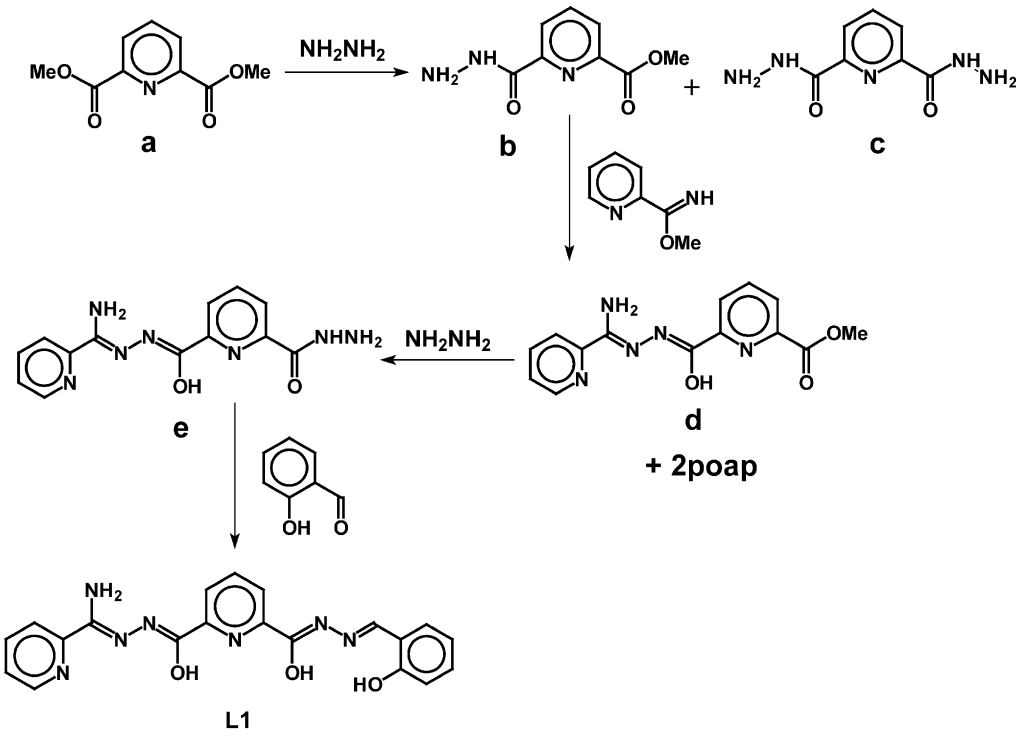

Scheme 2.

2.2.3. Iminodiacetic acid hydrazide ligand L3

The methyl ester of iminopicolinic acid was prepared in situ by reaction of 2-cyanopyridine (8.3 g, 80 mmol) and sodium methoxide solution, produced by dissolving sodium metal (0.23 g, 10 mmol) in dry methanol (50 ml). Iminodiacetic acid dihydrazide (3.2 g, 20 mmol), prepared by reaction of diethyl iminodiacetate (5.0 g, 26 mmol) with hydrazine hydrate (85%; 3.3 g, 56 mmol) in methanol/diethyl ether (1:1), was added to the above solution and the mixture gently refluxed for 1.5 h. A pale yellow precipitate formed, which was filtered off, washed with methanol and diethyl ether, and dried under vacuum (yield: 64%). m.p. 205–207 °C. Mass spectrum (major mass peaks, *m*/*z*): 333 [M−2H_2O], 174, 160, 105, 79 and 43. IR (Nujol mull, cm^{-1}): 3420 (s, *ν*(OH)), 3210 (m, *ν*(NH)), 1645 (s, *ν*(C=O), *ν*(C=N)), 997 (m, *ν*(py)). ^1H NMR (DMSO): $\delta = 8.57$ (m, 1H), 8.08 (m, 1H), 7.85 (m, 1H), 7.45 (m, 1H), 6.65 (dd, 2H), 3.60 (s, 1H). Elemental analysis: (L3) Anal. Found: C, 51.82; H, 5.28; N, 33.97. Calc. for $C_{16}H_{19}N_9O_2$: C, 52.02; H, 5.18; N, 34.12%.

2.3. Synthesis of the complexes

*2.3.1. [Cu_3(L1-3H)(CH_3COO)$_3$(H_2O)$_2$]·H_2O (**1**)*

L1 (0.10 g, 0.25 mmol) was added to a solution of copper acetate (0.32 g, 1.1 mmol) in methanol/water (50/50; 50 ml), and the mixture stirred until the ligand dissolved forming a clear green solution. The solution was filtered and allowed to stand at room temperature. Green rectangular plates suitable for structural analysis formed (yield: 45%). IR (cm^{-1}) 3320 (NH), 1689, 1635 (C=N, C=O), 1024 (py). UV–Vis (λ_{max}; nm) 696, 1474 (w). Elemental analysis: (**1**) Anal. Found: C, 37.72; H, 3.23; N, 11.77. Calc. for ($C_{20}H_{14}N_7O_3$)Cu_3(CH_3COO)$_3$·3H_2O: C, 37.84; H, 3.91; N, 11.88%.

*2.3.2. Cu_3(L1-3H)(NO_3)$_3$·3.5H_2O (**2**)*

L1 (0.10 g, 0.25 mmol) was added to a solution of $Cu(NO_3)_2$·3H_2O (0.32 g, 1.4 mmol) dissolved in a minimum volume of methanol. The mixture was heated with stirring and additional methanol added to just dissolve the precipitated solid and unreacted ligand. The hot clear green solution was filtered and left to stand at room temperature. Green crystals formed, which were filtered off, washed with methanol/ether and dried (yield: 60%). IR (cm^{-1}) 3631 (H_2O), 3195 (NH), 1672 (C=N, C=O), 1018 (py). UV–Vis (λ_{max}; nm) 695, 1480 (w). Elemental analysis: (**2**) Anal. Found: C, 28.60; H, 2.52; N, 16.63. Calc. for ($C_{20}H_{14}N_7O_3$)Cu_3(NO_3)$_3$·3.5H_2O: C, 28.59; H, 2.38; N, 16.67%.

*2.3.3. [Cu_3(L2-4H)(H_2O)$_3$(CH_3OH)](NO_3)$_2$ (**3**)*

L2 (0.500 g, 1.15 mmol) was added to a solution of $Cu(NO_3)_2$·3H_2O (3.00 g, 12.4 mmol) in methanol/water (20/5 ml) with warming. A green solution formed which deposited green crystals on standing (yield: 76%). IR (cm^{-1}) 3415 (H_2O), 1616 (C=N, C=O), 1005 (py). UV–Vis (λ_{max}; nm) 648, 1495 (w). Elemental analysis of **3**: Anal. Found: C, 31.62; H, 2.72; N, 11.89. Calc. for

$(C_{21}H_{13}N_5O_6)Cu_3(H_2O)_3(CH_3OH)(NO_3)_2$: C, 31.76; H, 2.79; N, 11.78%.

2.3.4. $Cu_3(L3\text{-}2H)(NO_3)_4\cdot 4.5H_2O$ (4)

L3 (0.0185 g, 0.500 mmol) was added to a solution of $Cu(NO_3)_2\cdot 3H_2O$ (0.50 g, 2.0 mmol) in methanol/dichloromethane (1:1) (30 ml) at room temperature. The ligand dissolved on stirring to give a deep blue clear solution. Slow evaporation of the solution at room temperature led to deep blue crystals, which were filtered off and dried in air (yield: 65%). IR (cm^{-1}) 3550 (ν(OH)), 3400, 3200 (ν(NH)), 1735 ($\nu(NO_3)$), 1665, 1675 (ν(C=O),ν(C=N)), 1020 (ν(py)). UV–Vis (nm) 650. Elemental analysis of **4**: Anal. Found: C, 21.86; H, 2.52; N, 20.29. Calc. for $(C_{16}H_{17}N_9O_2)Cu_3(NO_3)_4\cdot 4.5H_2O$: C, 21.66; H, 2.95; N, 20.53%.

2.3.5. $[Mn_3(L3)_2(CH_3CN)_2(H_2O)_2](ClO_4)_6\cdot 2H_2O$ (5)

L3 (0.10 g, 0.20 mmol) was added to a hot solution of $Mn(ClO_4)_2\cdot 6H_2O$ (0.21 g, 0.60 mmol) in acetonitrile (15 ml). After stirring for 10 min, the bright yellow solution was filtered. Slow evaporation at room temperature gave pale yellow crystals suitable for crystallographic analysis (yield: 60%). IR (cm^{-1}) 3436, 3426 (ν(OH)), 3352, 3259 (ν(NH)), 1636, 1615, 1585 (ν(C=O), ν(C=N)), 1084,1018 ($\nu(ClO_4)$). Elemental analysis of **5**: Anal. Found: C, 26.03; H, 3.06; N, 16.76. Calc. for $(C_{16}H_{19}N_9O_2)_2Mn_3(CH_3CN)_2(ClO_4)_6\cdot 4H_2O$: C, 26.13; H, 3.17; N, 16.93%.

2.3.6. $[Mn(L1)(NO_3)_2(H_2O)_2]\cdot 2H_2O$ (6)

L1 (0.10 g, 0.25 mmol) was suspended in chloroform/methanol (20/20 ml) and warmed. $Mn(NO_3)_2\cdot 6H_2O$ (0.36 g, 1.25 mmol) was added and the mixture warmed with stirring. A clear yellow solution formed, which was filtered and allowed to stand. A mixture of rectangular yellow crystals and crystals of the ligand formed, which were separated by hand (yield: $\sim$15%). The yellow crystals were found to be suitable for crystallographic analysis. No elemental analysis was performed.

2.4. X-ray crystallography

The diffraction intensities of a green prismatic crystal of **1** were collected with graphite-monochromatized Mo Kα X-radiation (rotating anode generator) using a Bruker P4/CCD diffractometer at 193(1) K to a maximum 2θ value of 52.8°. The data were corrected for Lorentz and polarization effects. The structure was solved by direct methods [8,9]. All atoms except hydrogen were refined anisotropically. Hydrogen atoms were placed in calculated positions with isotropic thermal parameters set to 20% greater than their bonded partners, and were not refined. Neutral atom scattering factors [10] and anomalous dispersion terms [11,12] were taken from the usual sources. All other calculations were performed with the TEXSAN [13] crystallographic software package using a PC computer. Crystal data collection and structure refinement for **3**, **5** and **6** were carried out in a similar manner using Mo Kα radiation. Abbreviated crystal data for **1**, **3**, **5** and **6** are given in Table 1.

3. Results and discussion

3.1. Structure of $[Cu_3(L1\text{-}3H)(CH_3COO)_3(H_2O)_2]\cdot H_2O$ (1)

The structure of **1** is illustrated in Fig. 1 and important bond lengths and angles are listed in Table 2. The fundamental unit is trinuclear with three square-pyramidal copper(II) centers bound to one unsymmetrical ligand in a *trans* arrangement (Scheme 1). Cu(1) is bound to the phenolic end of the ligand with a $CuNO_3$ basal plane (Cu–O, 1.923–2.012 Å; Cu(1)–N(1), 1.940(4) Å), and a long contact to water O(14) (2.286(4) Å). Cu(3) is bound to the pyridine end with a CuN_2O_2 basal plane (Cu–O, 1.923–1.994 Å; Cu–N, 1.909–2.003 Å), and a long axial contact to a bridging acetate (Cu–O, 2.309(4) Å). Cu(2) has a CuN_3O basal plane (Cu–N, 1.939–2.083 Å; Cu(2)–O(6), 1.937(3) Å) and a long axial contact to a bridging acetate (Cu(2)–O(9), 2.202(4) Å). The central copper (Cu(2)) is connected to both Cu(1) and Cu(3) via close to *trans*-N–N bridges (Cu–N–N–Cu torsional angles 161.4° and 163.6°) within each trinuclear subunit, leading to quite long Cu–Cu separations (Cu(2)–Cu(1), 4.831(2) Å; Cu(2)–Cu(3), 4.870(2) Å). Each trinuclear subunit forms a dimeric unit via axial connections to between Cu(1) and Cu(2) from terminal carboxylates bound to Cu(1), thus creating a hexanuclear secondary subunit (Fig. 1). This subunit forms a chain in the overall structure via axial contacts between Cu(3) and carboxylate oxygen O(10).

3.2. Structure of $[Cu_3(L2\text{-}4H)(H_2O)_3(CH_3OH)](NO_3)_2$ (3)

The structure of **3** is depicted in Fig. 2 and selected bond distances and angles are listed in Table 3. The ligand binds three Cu(II) centers in a linear trinuclear array, with no apparent connective interactions to neighboring molecules as are observed in **1**. Cu(2) is connected to Cu(1) and Cu(3) by almost *trans*-N–N diazine bridges (Cu(1)–N(1)–N(2)–Cu(2), 176.7°; Cu(2)–N(4)–N(5)–Cu(3), 172.1°; Cu(1)–Cu(2), 4.871(1) Å; Cu(2)–Cu(3), 4.887(2) Å). The central copper is square-pyramidal with an axially bound water and a tightly bound in plane water (Cu(2)–O(8), 2.181(2) Å; Cu(2)–O(9), 1.937(2) Å). Cu(1) and Cu(3)

Table 1
Crystal data and structure refinement parameters for compounds **1**, **3**, **5**, **6**

	1	**3**	**5**	**6**
Empirical formula	$C_{26}H_{29}N_7O_{12}Cu_3$	$C_{22}H_{23}N_7O_{16}Cu_3$	$C_{36}H_{52}N_{20}O_{32}C_{l6}Mn_3$	$C_{20}H_{22.2}N_{8.5}O_{10.6}Mn$
Formula weight	822.19	832.1	1654.45	606.18
Temperature (K)	190(1)	190(1)	190(1)	190(1)
Wavelength (Å)	0.71073	0.71073	0.71073	0.71073
Crystal system	monoclinic	monoclinic	monoclinic	monoclinic
Space group	$P2_1/c$	$P2_1/n$ (14)	$C2/c$ (15)	$C2/c$ (15)
Unit cell dimensions				
a (Å)	17.741(1)	10.0066(7)	14.957(2)	33.320(8)
b (Å)	13.4455(8)	20.576(1)	21.519(2)	10.524(2)
c (Å)	14.6271(9)	13.7619(9)	19.792(2)	16.611(4)
β (°)	108.267(1)	90.050(2)	103.233(2)	101.5990(5)
V (Å^3)	3313.3(3)	2833.6(3)	6201(1)	5706(2)
Z	4	4	4	8
D_{calc} (g cm^{-3})	1.648	1.950	1.772	1.411
μ (cm^{-1})	19.78	23.24	9.67	5.29
R_1	0.048	0.038	0.060	0.159
wR_2	0.161	0.092	0.169	0.437

$R_1 = \Sigma||F_0| - |F_c||/\Sigma|F_0|$, $wR_2 = \{\Sigma[w(F_0^2 - F_c^2)^2]/\Sigma[w(F_0^2)^2]\}^{1/2}$.

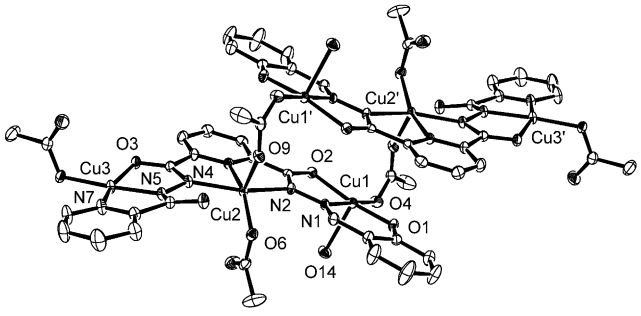

Fig. 1. Structural representation of **1** showing the associated dimeric hexanuclear unit (40% thermal ellipsoids).

have square-planar NO_3 coordination environments, with an equatorial water (O(10)) bound to Cu(3) and a methanol bound to Cu(1) (O(7)). Cu(1) is actually square-pyramidal with a distant contact to nitrate oxygen O(13) (Cu(1)–O(13), 2.637(2) Å). The second phenolic oxygens (O(2) and O(6)) are not involved in bonding, but certainly are poised for possible additional external coordination.

3.3. Structure of $[Mn_3(L3)_2(CH_3CN)_2(H_2O)_2](ClO_4)_6\cdot 2H_2O$ (**5**)

The structure of **5** is illustrated in Fig. 3 and selected bond distances and angles are listed in Table 4. The structure comprises three Mn(II) centers, arranged as a dinuclear oxygen bridged, $Mn_2(\mu\text{-}O)_2$, subunit, involving seven-coordinate, pentagonal-bipyramidal, Mn(II) centers, and a pseudo-octahedral mononuclear Mn(II) center. Two neutral ligands are involved in the trinuclear complex, arranged in a bent fashion with one end of each ligand bound to the dinuclear center, and the other end of each ligand bound to the mononuclear center. Protons have been located on N(4), N(5), N(6), and the symmetry-related nitrogen atoms, and the short C–O bond lengths (C(10)–O(2), 1.230(5) Å) to the bridging oxygen atoms indicate that they have significant C=O double bond character. The central nitrogen atoms (N(5)) form terminal bonds to Mn(2), and its symmetry-related partner, which is the point of bifurcation of each ligand. An acetonitrile is bonded to each dinuclear Mn(2) center in an axial position (Mn(2)–N(10), 2.208(4) Å), while two *cis*-coordinated water molecules complete the coordination sphere of Mn(1) (Mn(1)–O(15), 2.246(3) Å).

The Mn(2)–Mn(2_a) separation is 3.903(2) Å, and the Mn(1)–Mn(2) separation is 5.315(2) Å. Mn–O distances to the oxygen bridging atoms are quite long (Mn(2)–O(2), 2.235(3) Å; Mn(2_a)–O(2), 2.356(3) Å) in keeping with the neutral nature of the oxygen atoms themselves, and the large Mn–Mn separation. This leads to a large oxygen bridge angle, Mn(2)–O(2)–Mn(2_a), of 116.45(13)°. Other Mn–ligand distances are in the range 2.161–2.246 Å (Mn(1)) and 2.167–2.356 Å (Mn(2)), fairly typical for Mn(II).

3.4. Structure of $[Mn(L1)(NO_3)_2(H_2O)_2]\cdot 2H_2O$ (**6**)

The structure of **6** is shown in Fig. 4 and selected bond lengths and angles are listed in Table 5. This is a rather poorly refined structure, but the essential elements are clearly defined. The Mn(II) center is bonded to one external N_2O ligand pocket at the pyridine end of the ligand. Mn(1) has an unusual pentagonal-bipyramidal (MnN_2O_5) geometry, with three ligand donors (N_2O) and a bidentate chelating nitrate in the equatorial plane, and two axial water molecules (see [14] for other

Table 2
Selected bond lengths (Å) and bond angles (°) for compound **1**

Bond lengths	
Cu(1)–O(1)	1.924(4)
Cu(1)–O(2)	2.012(4)
Cu(1)–O(4)	1.923(4)
Cu(1)–O(14)	2.286(4)
Cu(1)–N(1)	1.940(4)
Cu(2)–O(6)	1.937(3)
Cu(2)–O(9)	2.202(4)
Cu(2)–N(2)	2.056(4)
Cu(2)–N(3)	1.939(4)
Cu(2)–N(4)	2.083(4)
Cu(3)–O(3)	1.994(3)
Cu(3)–O(10)	2.309(4)
Cu(3)–N(5)	1.909(4)
Cu(3)–N(7)	2.003(4)
Cu(3)–O(10_a)	1.923(4)
N(4)–N(5)	1.402(6)
Bond angles	
O(1)–Cu(1)–O(2)	167.91(17)
O(1)–Cu(1)–O(4)	90.17(16)
O(1)–Cu(1)–O(14)	99.45(16)
O(1)–Cu(1)–N(1)	92.50(17)
O(2)–Cu(1)–O(4)	96.74(15)
O(2)–Cu(1)–O(14)	90.90(14)
O(2)–Cu(1)–N(1)	80.88(15)
O(4)–Cu(1)–O(14)	86.37(14)
O(4)–Cu(1)–N(1)	176.96(16)
O(14)–Cu(1)–N(1)	91.75(16)
O(6)–Cu(2)–O(9)	87.99(14)
O(6)–Cu(2)–N(2)	100.90(15)
O(6)–Cu(2)–N(3)	156.96(17)
O(6)–Cu(2)–N(4)	99.18(15)
O(9)–Cu(2)–N(2)	100.27(14)
O(9)–Cu(2)–N(3)	114.87(15)
O(9)–Cu(2)–N(4)	88.62(15)
N(2)–Cu(2)–N(3)	78.74(16)
N(2)–Cu(2)–N(4)	158.27(16)
N(3)–Cu(2)–N(4)	79.53(16)
O(3)–Cu(3)–O(10)	102.27(15)
O(3)–Cu(3)–N(5)	80.66(16)
O(3)–Cu(3)–N(7)	159.58(16)
O(3)–Cu(3)–O(10_a)	97.19(16)
O(10_a)–Cu(3)–N(5)	176.46(18)
O(10)–Cu(3)–N(5)	105.15(15)
O(10_a)–Cu(3)–N(7)	100.71(17)
O(10)–Cu(3)–N(7)	91.05(16)
O(10)–Cu(3)–O(10_a)	78.01(15)
N(5)–Cu(3)–N(7)	80.95(17)
Cu(3)–O(10)–Cu(3_a)	101.99(1)

seven-coordinate examples). In plane, distances range from 2.24 to 2.37 Å with shorter axial contacts (Mn(1)–O(4), 2.162(11) Å; Mn(1)–O(5), 2.143(8) Å). The central ligand cavity appears to be occupied by a weakly hydrogen bonded nitrate, with weak hydrogen bonding contacts between O(9), and N(6) and N(2) (3.015 and 2.947 Å, respectively). The overall structure bears a striking resemblance to the mononuclear Fe(III) complex [Fe(H-poap-H)(NO_3)(H_2O)$_2$](NO_3)$_2$ [15], where the seven-coordinate Fe(III) center is bound in exactly the same manner to one N_2O coordination pocket of the ligand poap, with a chelating in plane bidentate nitrate and two axial waters. The Fe(III) ligand distances are generally shorter, as would be expected. The occupation of the ligand nitrogen-rich site only, despite an excess of metal during preparation of **6**, might indicate a preference based on donor composition and the combination of chelate rings involved.

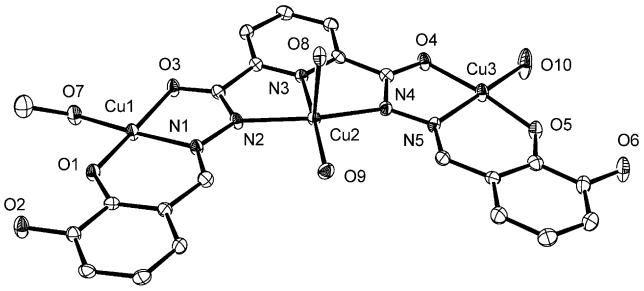

Fig. 2. Structural representation of **3** (40% thermal ellipsoids).

Table 3
Selected bond lengths (Å) and bond angles (°) for compound **3**

Bond lengths	
Cu(1)–O(1)	1.873(2)
Cu(1)–O(3)	1.945(2)
Cu(1)–O(7)	1.955(2)
Cu(1)–N(1)	1.933(3)
Cu(2)–O(8)	2.181(2)
Cu(2)–O(9)	1.937(2)
Cu(2)–N(2)	2.073(3)
Cu(2)–N(3)	1.935(3)
Cu(2)–N(4)	2.095(3)
Cu(3)–O(4)	1.942(2)
Cu(3)–O(5)	1.870(2)
Cu(3)–O(10)	1.920(3)
Cu(3)–N(5)	1.930(3)
N(1)–N(2)	1.400(4)
N(4)–N(5)	1.399(4)
Bond angles	
O(1)–Cu(1)–O(3)	173.95(9)
O(1)–Cu(1)–O(7)	92.21(10)
O(1)–Cu(1)–N(1)	94.73(10)
O(3)–Cu(1)–O(7)	90.95(10)
O(3)–Cu(1)–N(1)	82.41(11)
O(7)–Cu(1)–N(1)	172.46(11)
O(8)–Cu(2)–O(9)	92.16(9)
O(8)–Cu(2)–N(2)	96.84(10)
O(8)–Cu(2)–N(3)	96.27(11)
O(8)–Cu(2)–N(4)	95.42(10)
O(9)–Cu(2)–N(2)	99.44(10)
O(9)–Cu(2)–N(3)	171.55(11)

3.5. Magnetic properties

The fundamental repeat unit in **1** is trinuclear, with the basal planes of the $d_{x^2-y^2}$ ground-state copper centers connected by almost *trans*-N–N bridges. This should lead to quite strong antiferromagnetic coupling based on

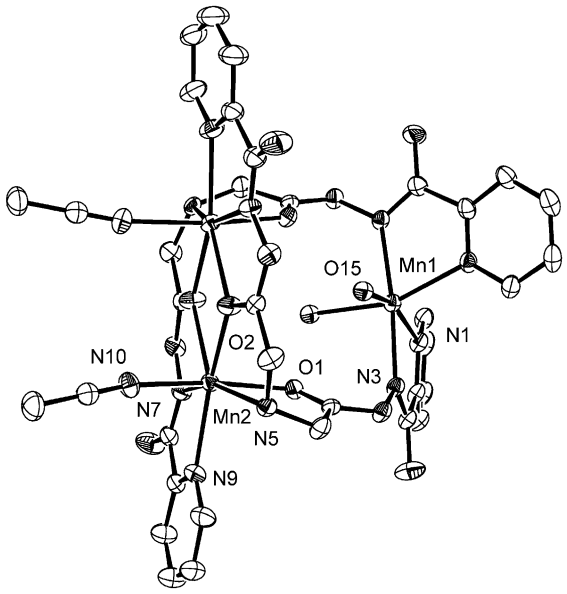

Fig. 3. Structural representation of **5** (40% thermal ellipsoids).

previous studies with similar bridges [6,7,16–18]. The connections that link the subunits together are all axial and strictly orthogonal with respect to magnetic connections between the copper centers. This being the case a simple trinuclear exchange model was used to fit the variable temperature magnetic data for **1**, based on the Hamiltonian described in Eq. (1). The spin states and

$$H_{ex} = -2J(S_1S_2 + S_2S_3) \quad (1)$$

$$\chi_{M'} = \frac{N\beta^2 g^2}{3k(T-\theta)} \left(\frac{\sum S_T(S_T+1)(2S_T+1)\, e^{-E(S_T)/kT}}{\sum (2S_T+1)\, e^{-E(S_T)/kT}} \right) \quad (2)$$

$$\chi_M = \chi_{M'}(1-\rho) + \frac{4S(S+1)N\beta^2 g^2 \rho}{3kT} + \mathrm{TIP} \quad (3)$$

their energies were calculated by the normal Kambe spin vector coupling approach [19], and substituted into the Van Vleck equation (Eq. (2)) in the normal way to generate the exchange expression (Eq. (1); $S = 1/2$). This was achieved within a generalized software package (MAGMUN4.0), which allows input of the metal ion spin states, and the direct exchange model, and fits the experimental variable temperature magnetic data via a weighted nonlinear regression procedure [20]. Corrections for θ (Weiss-like correction for intermolecular exchange effects; Eq. (2)), paramagnetic impurity fraction (ρ) and TIP (temperature-independent paramagnetism; Eq. (3)) are also included. Fig. 5 shows the experimental profile of μ_{mol} data as a function of temperature, with a drop in moment from $2.95\mu_B$ at 300 K to a plateau value of $1.8\mu_B$ at low temperature, typical of a trinuclear Cu(II) system. The solid line in Fig. 5 shows the good data fit for $g = 2.134(5)$, $-2J = 124(1)$ cm^{-1}, TIP $= 0.000200$ cm^3 mol^{-1}, $\rho = 0$, $\theta = -0.6$ K ($10^2R = 0.48$; $R = [\Sigma(\chi_{obs} - \chi_{calc})^2/\chi^2_{obs}]^{1/2}$). The small negative θ value indicates some weak intermolecular association undoubtedly due to the subunit con-

Table 4
Selected bond lengths (Å) and angles (°) for compound **5**

Bond lengths	
Mn(1)–O(15)	2.246(3)
Mn(1)–N(1)	2.232(3)
Mn(1)–N(3)	2.161(3)
Mn(2)–O(1)	2.167(3)
Mn(2)–O(2)	2.235(3)
Mn(2)–N(7)	2.244(3)
Mn(2)–N(9)	2.334(4)
Mn(2)–N(10)	2.208(4)
Mn(2)–O(2_a)	2.356(3)
N(3)–N(4)	1.404(5)
N(6)–N(7)	1.389(5)
Bond angles	
O(15)–Mn(1)–N(1)	160.02(12)
O(15)–Mn(1)–N(3)	86.97(12)
O(15)–Mn(1)–O(15_a)	91.43(12)
O(15)–Mn(1)–N(1_a)	87.68(12)
O(15)–Mn(1)–N(3_a)	88.57(12)
N(1)–Mn(1)–N(3)	73.05(12)
O(15_a)–Mn(1)–N(1)	87.68(12)
N(1)–Mn(1)–N(1_a)	99.81(12)
N(1)–Mn(1)–N(3_a)	111.29(12)
O(15_a)–Mn(1)–N(3)	88.57(12)
N(1_a)–Mn(1)–N(3)	111.29(12)
N(3)–Mn(1)–N(3_a)	173.62(13)
O(15_a)–Mn(1)–N(1_a)	160.02(12)
O(15_a)–Mn(1)–N(3_a)	86.97(12)
N(1_a)–Mn(1)–N(3_a)	73.05(12)
O(1)–Mn(2)–O(2)	90.93(12)
O(1)–Mn(2)–N(7)	91.89(12)
O(1)–Mn(2)–N(9)	90.84(12)
O(1)–Mn(2)–N(10)	166.40(13)
O(1)–Mn(2)–O(2_a)	96.89(11)
O(2)–Mn(2)–N(7)	130.29(12)
O(2)–Mn(2)–N(9)	160.23(13)
O(2)–Mn(2)–N(10)	87.14(15)
O(2)–Mn(2)–O(2_a)	63.54(10)
N(7)–Mn(2)–N(9)	69.31(14)
N(7)–Mn(2)–N(10)	99.62(15)
O(2_a)–Mn(2)–N(7)	66.85(12)
N(9)–Mn(2)–N(10)	86.53(15)
O(2_a)–Mn(2)–N(9)	135.66(13)
O(2_a)–Mn(2)–N(10)	94.29(13)
Mn(2)–O(2)–Mn(2_a)	116.45(13)

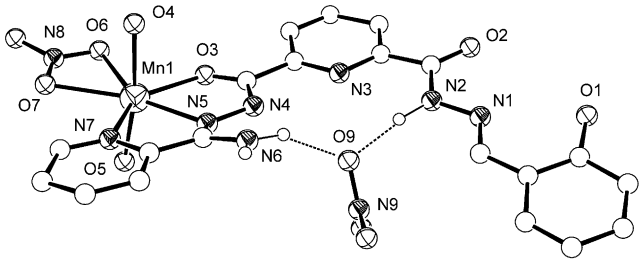

Fig. 4. Structural representation of **6**.

Table 5
Selected bond lengths (Å) and bond angles (°) for compound **6**

Bond lengths	
Mn(1)–O(3)	2.247(8)
Mn(1)–O(4)	2.162(11)
Mn(1)–O(5)	2.143(8)
Mn(1)–O(6)	2.309(9)
Mn(1)–O(7)	2.362(8)
Mn(1)–N(5)	2.252(8)
Mn(1)–N(7)	2.297(9)
N(1)–N(2)	1.400(11)
N(4)–N(5)	1.370(11)
Bond angles	
O(3)–Mn(1)–O(4)	90.8(4)
O(3)–Mn(1)–O(5)	91.3(3)
O(3)–Mn(1)–O(6)	80.2(3)
O(3)–Mn(1)–O(7)	135.2(3)
O(3)–Mn(1)–N(5)	69.5(3)
O(3)–Mn(1)–N(7)	139.8(3)
O(4)–Mn(1)–O(5)	169.1(4)
O(4)–Mn(1)–O(6)	83.2(4)
O(4)–Mn(1)–O(7)	85.8(3)
O(4)–Mn(1)–N(5)	90.6(4)
O(4)–Mn(1)–N(7)	88.2(4)
O(5)–Mn(1)–O(6)	86.7(3)
O(5)–Mn(1)–O(7)	85.2(3)
O(5)–Mn(1)–N(5)	100.2(3)
O(5)–Mn(1)–N(7)	97.1(3)
O(6)–Mn(1)–O(7)	55.0(3)
O(6)–Mn(1)–N(5)	148.9(3)
O(6)–Mn(1)–N(7)	139.4(4)
O(7)–Mn(1)–N(5)	155.0(3)
O(7)–Mn(1)–N(7)	84.9(3)
N(5)–Mn(1)–N(7)	70.3(3)

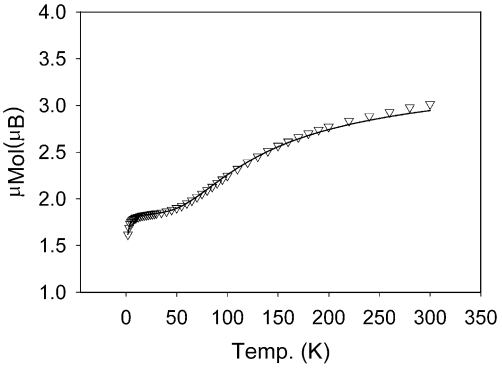

Fig. 5. Plot of magnetic moment (μ_{mol}) versus temperature for **1**. The solid line was calculated from Eq. (1) for $g = 2.134(5)$, $-2J = 124(1)$ cm^{-1}, TIP = 0.000200 cm^3 mol^{-1}, $\rho = 0$, $\theta = -0.6$ K ($10^2R = 0.48$).

nections apparent in the overall chain structure. The exchange integral is typical for systems of this sort with close to *trans*-N–N bridging connections [6,7]. Compound **2** has an almost identical μ_{mol}/T profile with a very good data fit to Eq. (1) ($S = 1/2$) for $g = 2.29(1)$, $-2J = 159(3)$ cm^{-1}, TIP = 0.000400 cm^3 mol^{-1}, $\rho = 0.065$, $\theta = -0.4$ K ($10^2R = 1.8$). This suggests a similar subunit structure with three Cu(II) centers bound to a single ligand in a similar fashion to **1**. The slightly larger exchange coupling probably signifies a larger Cu–N–N–Cu torsional angle. No structural details are yet available for this compound.

Compound **3** also behaves as a typical linear trinuclear Cu(II) system, with a room temperature moment of $3.2\mu_B$ dropping to $1.9\mu_B$ at 2 K, indicative of an $S = 1/2$ ground state. Successful fitting of the magnetic data to Eq. (1) gave $g = 2.21(1)$, $-2J = 117(3)$ cm^{-1}, TIP = 0.000300 cm^3 mol^{-1}, $\rho = 0.0003$, $\theta = 0$ ($10^2R = 1.6$). Again this moderate antiferromagnetic exchange is consistent with the close to *trans* arrangement of the copper centers about the N–N single bonds. Compound **4** behaves in an identical manner magnetically fitting extremely well to Eq. (1) ($S = 1/2$) with g = 2.244(4), $-2J = 161(1)$ cm^{-1}, TIP = 0.000145 cm^3 mol^{-1}, $\rho = 0.0108$, $\theta = -0.12$ K ($10^2R = 0.25$). This clearly indicates a linear trinuclear structure, with an exchange integral typical for a *trans*-N–N-bridged system, which would be anticipated as one likely coordination possibility for ligand L3, which has a similar overall 'bite' to 2-poap, L1 and L2.

The profile of magnetic susceptibility (χ per mol) as a function of temperature for **5** is shown in Fig. 6. The value at 300 K corresponds to a magnetic moment per mole of $10.5\mu_B$, which drops to $5.7\mu_B$ at 2 K, indicative of the presence of significant antiferromagnetic coupling in a dinuclear $Mn(II)_2$ subunit, and an essentially isolated mononuclear Mn(II) center. The magnetic data were fitted to a model including an

$$H = -2J\{S_1 + S_2\} + S_3 \quad (4)$$

exchange coupled dinuclear center, and an isolated mononuclear center (Eq. (4); $S_1 = S_2 = S_3 = 5/2$) using MAGMUN4.0 [20]. A reasonable data fit was obtained for $g_{av} = 2.05(1)$, $2J = -5.6(2)$ cm^{-1}, $\rho = 0.0055$, TIP = 0 cm^3 mol^{-1}, $\theta = -0.5$ K ($10^2R = 2.2$). The solid line in Fig. 6 was calculated with these parameters. The moderate exchange integral for **5** is consistent with the fairly large Mn–O–Mn angle of 116.5° [21,22]. How-

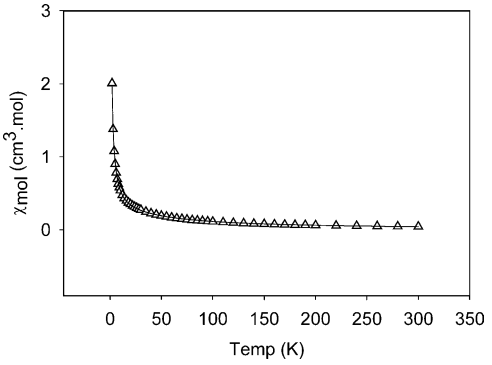

Fig. 6. Plot of magnetic susceptibility moment (χ_{mol}) versus temperature for **5**. The solid line was calculated from Eq. (2) for $g = 2.05(1)$, $-2J = 5.6(2)$ cm^{-1}, TIP = 0 cm^3 mol^{-1}, $\rho = 0.0055$, $\theta = -0.5$ K ($10^2R = 2.2$).

ever, this is an unusual case because of the fairly long Mn–O bridge contacts and the ketonic character of the CO bond. The mononuclear compound **6** has an essentially constant magnetic moment from 300 to 20 K ($6.0\mu_B$), typical of a mononuclear species, which then drops slightly below 20 K possibly due to zero-field splitting.

4. Conclusions

Three new tritopic ligands are reported along with some trinuclear complexes. The unsymmetric and symmetric ligands L1 and L2 are based on a central 2,6-pyridine dicarboxylate core, with the L1 synthesis possible because of the difference in solubility between the half hydrazide (d in Scheme 1) and the symmetric tritopic ligand 2-poap. The tritopic ligand L3, based on the iminodiacetic acid hydrazide core, is an important new member in this class, with much more internal flexibility, and it is reasonable to assume that in the case of the copper complex **4** it behaves as a linear trinucleating ligand. The structures of **1** and **3** reveal a *trans* arrangement of the three-ligand pockets, leading to *trans*-N–N bridged complexes. The magnetic consequences of this bridging arrangement are shown clearly with good fitting of the data to a linear trinuclear exchange expression with moderately large $-2J$ values typical of this bridging structure.

Compound **5** has a most unusual 2+1 trinuclear structure, with an antiferromagnetically coupled $Mn_2(\mu\text{-}O)_2$ dinuclear center involving neutral carbonyl oxygen bridges. Further studies on the complexes of these ligands are ongoing.

5. Supplementary material

Crystallographic data for the structural analyses have been deposited with the Cambridge Crystallographic Data Center, CCDC Nos. 196495–196498. Copies of this information may be obtained free of charge from The Director, CCDC, 12 Union Road, Cambridge, CB2 1EZ, UK (Fax: +44-1223-336033; e-mail: deposit@ccdc.cam.ac.uk or http://www.ccdc.cam.ac.uk).

Acknowledgements

This study was supported by the Natural Sciences and Engineering Research Council of Canada (NSERC). We thank Dr. R. McDonald, University of Alberta, for structural data.

References

[1] L. Zhao, Z. Xu, L.K. Thompson, D.O. Miller, Polyhedron 20 (2001) 1359.
[2] L. Zhao, Z. Xu, L.K. Thompson, S.L. Heath, D.O. Miller, M. Ohba, Angew. Chem., Int. Ed. Engl. 39 (2000) 3114.
[3] L. Zhao, C.J. Matthews, L.K. Thompson, S.L. Heath, J. Chem. Soc., Chem. Commun. (2000) 265.
[4] O. Waldmann, R. Koch, S. Schromm, P. Müller, L. Zhao, L.K. Thompson, Chem. Phys. Lett. 332 (2000) 73.
[5] O. Waldmann, L. Zhao, L.K. Thompson, Phys. Rev. Lett. 88 (2002) 066401.
[6] L. Zhao, L.K. Thompson, Z. Xu, D.O. Miller, D.R. Stirling, J. Chem. Soc., Dalton Trans. (2001) 1706.
[7] X. Chen, S. Zhan, C. Hu, Q. Meng, Y. Liu, J. Chem. Soc., Dalton Trans. (1997) 245.
[8] (a) G.M. Sheldrick, SHELX-97, 1997.;
(b) A. Altomare, M. Cascarano, C. Giacovazzo, A. Guagliardi, J. Appl. Cryst. 26 (1993) 343.
[9] P.T. Beurskens, G. Admiraal, G. Beurskens, W.P. Bosman, R. de Gelder, R. Israel, J.M.M. Smits, The DIRDIF-94 Program System: Technical Report of the Crystallography Laboratory, University of Nijmegen, The Netherlands, 1994.
[10] D.T. Cromer, J.T. Waber, International Tables for X-ray Crystallography, vol. IV (Table 2.2A), Kynoch, Birmingham, 1974.
[11] J.A. Ibers, W.C. Hamilton, Acta Crystallogr. 17 (1964) 781.
[12] D.C. Creagh, W.J. McAuley, in: A.J.C. Wilson (Ed.), International Tables for Crystallography, vol. C (Table 4.2.6.8), Kluwer Academic Publishers, Boston, MA, 1992, pp. 219–222.
[13] TEXSAN for Windows: Crystal Structure Analysis Package, Molecular Structure Corporation, The Woodlands, TX, 1997.
[14] A. Bianchi, L. Calabi, C. Giorgi, P. Losi, P. Mariani, D. Palano, P. Paoli, P. Rossi, B. Valtancoli, J. Chem. Soc., Dalton Trans. (2001) 917, and references cited therein.
[15] Z. Xu, L.K. Thompson, C.J. Matthews, D.O. Miller, A.E. Goeta, J.A.K. Howard, Inorg. Chem. 40 (2001) 2446.
[16] Z. Xu, L.K. Thompson, D.O. Miller, Inorg. Chem. 36 (1997) 3985.
[17] L.K. Thompson, Z. Xu, A.E. Goeta, J.A.K. Howard, H.J. Clase, D.O. Miller, Inorg. Chem. 37 (1998) 3217.
[18] Z. Xu, L.K. Thompson, D.O. Miller, H.J. Clase, J.A.K. Howard, A.E. Goeta, Inorg. Chem. 37 (1998) 3620.
[19] K. Kambe, J. Phys. Soc. Jpn. 5 (1950) 38.
[20] MAGMUN4.0 is available free of charge. We do not distribute the source codes. The programs may be used only for scientific purposes, and economic utilization is not allowed. If the routine is used to obtain scientific results, which are published, the origin of the programs should be quoted. Access at http://www.chem.-mun.ca/C-CART/squidpage.php or from lthomp@mun.ca.
[21] H.-R. Chang, K. Larsen, P.D.W. Boyd, C.G. Pierpont, D.N. Hendrickson, J. Am. Chem. Soc. 110 (1988) 4565.
[22] S.-B. Yu, C.-P. Wang, E.P. Day, R.H. Holm, Inorg. Chem. 30 (1991) 4067.